KSME

Springer

Journal of Mechanical Science and Technology 34 (1) 2020

Original Article
DOI 10.1007/s12206-019-1044-0

Keywords:
· Computational fluid dynamics
· Forced convection
· Heat transfer
· Oval tube
· Pressure drop
· Vortex generators

Correspondence to:
Md. Ashiqur Rahman
ashiqurrahman@me.buet.ac.bd

Citation:
Haque, M. R., Rahman, M. A. (2020). Numerical investigation of convective heat transfer characteristics of circular and oval tube banks with vortex generators. Journal of Mechanical Science and Technology 34 (1) (2020) 457-467.
http://doi.org/10.1007/s12206-019-1044-0

Received February 9th, 2019
Revised July 1st, 2019
Accepted September 18th, 2019

† Recommended by Editor
Yong Tae Kang

© The Korean Society of Mechanical Engineers and Springer-Verlag GmbH Germany, part of Springer Nature 2020

Numerical investigation of convective heat transfer characteristics of circular and oval tube banks with vortex generators

Mohammad Rejaul Haque[1] and Md. Ashiqur Rahman[2]

[1]Mechanical and Production Engineering, Ahsanullah University of Science & Technology, Dhaka-1208, Bangladesh, [2]Department of Mechanical Engineering, Bangladesh University of Engineering and Technology (BUET), Dhaka-1000, Bangladesh

Abstract The present work represents a 3-D numerical investigation of forced convection heat transfer over circular and oval tube banks with longitudinal vortex generators (LVGs) for flow through a fin-and-tube heat exchanger. The thermo-hydraulic performance parameters are studied numerically using computational fluid dynamics (CFD) tool. It is found that within the range of Reynolds number (500-850) studied, the degree of heat transfer enhancement is greatly influenced by the tube shape. Heat transfer increases by 13 % when the angle of attack is varied from 15º to 25º, with a corresponding pressure drop of 40 % and 62 % for the oval tubes and circular tubes, respectively. The effect of the aspect ratio of the oval tubes is observed to be very significant. Several other performance parameters of the oval and circular tube banks with vortex generators under the same operating conditions are compared with a focus on finding an optimal configuration.

1. Introduction

Heat exchangers (HE) are used for numerous areas of application. Hence, it is always desired to increase the efficiency of heat exchange devices to save energy as well as cost. Finding design improvements of heat exchangers to enhance their performance has for long received the attention of researchers because of their tremendous technical importance [1]. It is widely accepted that the enhancement of heat transfer obtained from the introduction of vortex generators (VG) of different types and shapes and configurations (longitudinal, transverse, curved, inclined, etc.) in channel flow is principally due few common mechanisms, explained elaborately by Tiggelbeck et al. [2]. These mechanisms include the generation of a secondary flow consisting of interacting vortices, development of three-dimensional turbulent boundary layer, and thinning of the sub-laminar boundary layer at the wall.

Longitudinal vortex generators (LVGs), capable of generating interacting vortices or swirl flow along the flow direction, have received considerable attention from the researchers from the last two decades and have been studied for the air- or gas-side heat transfer augmentation of different types of HE. Fiebig [3, 4] reported that LVGs can significantly increase the heat transfer coefficient in laminar channel flows and can realize more significant heat transfer enhancement than the transverse VGs. An increase of 55- 65 % in the heat transfer coefficient with an associated pressure drop increase of 20-45 % for inline tube arrangement was reported. The findings of an experimental study on the heat and momentum transfer in a turbulent channel flow with LVGs were reported by Lau et al. [5].

The effect of installing vortex generators on different types of HE (fin-and tube, louvered) under different operating conditions (dry, wet and frosting) was studied and reported by several researchers, both experimentally and numerically [6-16]. The effects of using different types and configurations of VGs in flow fields with oval tube or tube array have also been examined

widely [17-26]. Oval tubes have certain advantages in terms of pressure drop reduction and smaller wake zone over the circular tubes. Therefore, when LVG is used in combination with oval tubes, better thermal performance can be obtained without a substantial increase in the pressure drop [17]. Chen and Fiebig numerically studied the effect of the aspect ratio of tubes, angle of attack and arrangement of multiple VGs on the thermal-hydraulics performance of fin-and-oval-tube HE in the staggered and inline configuration of tubes [18-20]. They found the staggered configuration of the winglets to be more efficient in heat transfer augmentation than the inline winglet arrangement because the longitudinal vortices in the staggered winglet arrangement were found to affect a larger flow area and intensify the secondary flow. In a similar numerical study, Tiwari et al. [21] examined the effect of the number of delta-winglet pairs on the thermal performance of fin-and-oval-tube HE and observed a considerable increase in Nusselt number as more delta-winglet pairs, in both inline and staggered arrangement, were introduced in the flow field.

Prabhakar et al. [22, 23] reported the numerical study of heat transfer in a rectangular channel flow, simulating the single flow passage in a fin-and-tube HE, with built-in oval tube and different shape and arrangements of LVGs. The combination of the oval tube and delta-winglet was found to provide the optimum thermal performance, without a significant difference in the pressure drop than the circular tube case. In a couple of highly germane studies, the local heat transfer and pressure drop characteristics for flow in a rectangular channel (Re = 600-6500) with oval tube and delta-winglet VG was reported by O'Brien et al. [24, 25]. A local heat transfer enhancement of about 38 % was obtained for the combination of a single winglet pair and oval-tube compared to the oval-tube without-winglet case. In a recent study, the effects of angle of attack and the distance of the delta-winglet VGs from the center of the tube on the fluid-flow structure and heat transfer characteristics in a fin-and-oval-tube HE was examined numerically [26].

In recent years, researchers have explored few other possible areas of heat transfer enhancement using vortex generators, such as placing geometric features such as protrusions, dimples, punched delta winglet vortex generator, and inserts of different shapes in addition to VGs [27-29], using combined vortex generators [30], delta winglets with nanofluids [31], using built-in Interrupted delta-winglet [32], applying VGs in HE of different types [33, 34], wing-shaped tubes [35, 36], staggered wing shaped tubes [37, 38], double V-cut twisted tape inserts [39], ball-type turbulators [40], and reported encouraging findings. Heat transfer enhancement was reported for a range of angle of attack from 0° to 45º, while heat transfer decreases for angle of attack in the range of 135º-180º [37]. The effect of the geometric shape of the vortex generators on the thermo-hydraulic performance has also been studied widely in the recent years [41-44] to obtain an optimal shape for the maximum heat transfer enhancement with reduced pressure drop. The different geometric shapes that have been studied include elliptical, curved, angular, trapezoidal, and wavy. Detailed thermal performance and high-temperature application of heat exchangers were reported [45, 46] where insertion of VG with different tube shape could be an added advantage. The potential integration of VG with flat-plate solar water heater has also been studied [47].

Very little study, except probably the work of Prabhakar et al. [21, 22] and O'Brien et al. [24] for a limited scope, could be located in the open literature comparing the effect of VGs on the heat transfer and pressure drop characteristics of circular and oval tube banks under the same operating conditions. There is an apparent lack of understanding on how the thermo-hydraulic performance of multi-row fin-and-tube ex-changer with VG compare with circular and oval tubes having a similar cross-sectional area. Hence, the potential advantage of oval tubes is considered in reducing the form drag compared to circular-shaped tubes. In the study, the fluid-flow structure and heat transfer characteristics of a seven-row fin-and-tube HE with VGs in all tube-rows are examined in detail for both circular and oval tube banks and findings are reported.

2. Model and methods

2.1 Physical model

The geometry of a seven-row fin-and-tube HE is considered for the computational domain. The values of fin spacing and tube size, which are most commonly employed in the industrial system, have been selected in the present model. The computational domain considered in this study is of a channel of height H = 3.63 mm, width W = 25.4 mm, and L = 177.8 mm as shown in Figs. 1 and 2. The outside diameter of the tube is 10.67 mm; the fin thickness is minimal and is neglected. In case of oval tubes, the cross-sectional area of the tube is same to that of circular tubes and the major and the minor radius are calculated based on dif-ferent aspect ratios of the oval tubes as denoted by Fig. 3. The position of the winglet is fixed concerning the tip circumference of the circular and oval tubes.

In the present study, the dimensions of winglets are taken as length, l = 10.67 mm, width, w = 2.18 mm and thickness, ∂ = 0.18 mm. The winglets could be arranged as common flow up (CFU) and common flow down (CFD) configuration. The ratio of the major radius (b) to the minor radius (a) of the oval tube is termed as aspect ratio (AR) and the numerical investigation was carried out for different aspect ratios of the oval tubes for the stated conditions. Most of the results in the present study are for aspect ratio AR = 1.24, 1.54, 1.8, and 2.32, for oval tubes as shown in Fig. 4. Each VG attached on the bottom fin could rotate around the axis. The angle of attack α of the winglets is varied by 15º and 25º.

2.2 Governing equations and boundary conditions

In developing the model, the assumptions which have been considered are- steady-state, constant properties of fluid (*i.e.,* density, ρ; viscosity, μ; specific heat, *Cp*; and thermal conduc-

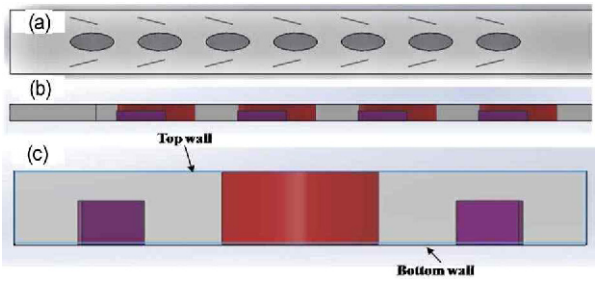

Fig. 1. Orthographic views of the computational domain with common flow up (CFU) configuration of winglets: (a) Top view; (b) side view; (c) front view.

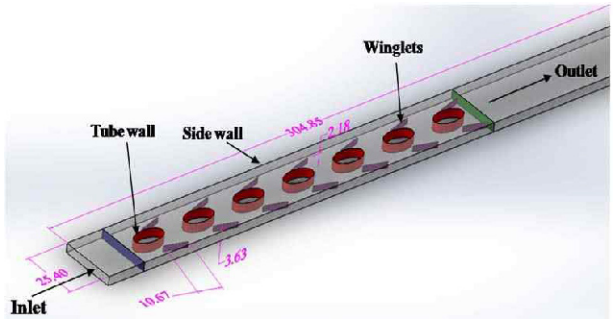

Fig. 2. Schematic diagram of the computational domain for oval tubes with common flow down (CFD) configuration of winglets.

tivity, K_f), incompressible flow, negligible viscous dissipation, and body force. The working fluid is air with constant properties (ρ = 1.225 Kg/m^3, μ = 1.789×10^{-5} Kg/m^3, C_p = 1006.43 J/Kg-K, and K_f = 0.0242 W/m-K). The flow is considered Laminar and steady (low inlet velocity and small height of the channel) similar to the Ref. [11] as well as the generation of the vortices is considered to be a quasi-steady phenomenon [48]. The compact forms of the governing equations Eqs. (1)-(5) can be written (generally) as follows:

Continuity equation:

$$\frac{\partial u}{\partial x}+\frac{\partial v}{\partial y}+\frac{\partial w}{\partial z}=0 \quad (1)$$

Momentum equations:

X-momentum:

$$\rho[u\frac{\partial u}{\partial x}+v\frac{\partial u}{\partial y}+w\frac{\partial u}{\partial z}]=-\frac{\partial p}{\partial x}+\mu[\frac{\partial^2 u}{\partial x^2}+\frac{\partial^2 u}{\partial y^2}+\frac{\partial^2 u}{\partial z^2}] \quad (2)$$

Y-momentum:

$$\rho[u\frac{\partial v}{\partial x}+v\frac{\partial v}{\partial y}+w\frac{\partial v}{\partial z}]=-\frac{\partial p}{\partial y}+\mu[\frac{\partial^2 v}{\partial x^2}+\frac{\partial^2 v}{\partial y^2}+\frac{\partial^2 v}{\partial z^2}] \quad (3)$$

Z-momentum:

$$\rho[u\frac{\partial w}{\partial x}+v\frac{\partial w}{\partial y}+w\frac{\partial w}{\partial z}]=-\frac{\partial p}{\partial z}+\mu[\frac{\partial^2 w}{\partial x^2}+\frac{\partial^2 w}{\partial y^2}+\frac{\partial^2 w}{\partial z^2}] \quad (4)$$

Table 1. Boundary conditions of the computational model.

Segment	Boundary conditions	
	Fluid	Energy
Inlet	Velocity	310.6 K
Tube wall	No slip	291.7 K
Side walls	Symmetry	Symmetry
Top wall	Symmetry	Symmetry
Bottom wall	Periodic	Periodic
Winglets	No slip	Adiabatic
Outlet	Pressure	Adiabatic

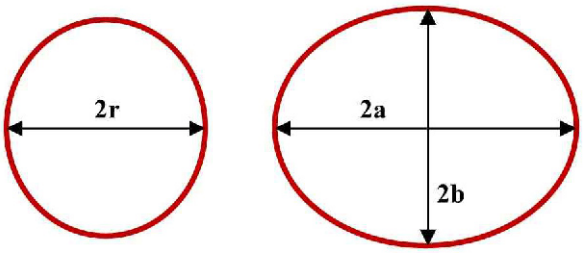

Fig. 3. Schematic of the tube region of a heat exchanger for (a) circular tube; (b) oval tube.

Energy equation:

$$\rho c_p[u\frac{\partial T}{\partial x}+v\frac{\partial T}{\partial y}+w\frac{\partial T}{\partial z}]=k_f[\frac{\partial^2 T}{\partial x^2}+\frac{\partial^2 T}{\partial y^2}+\frac{\partial^2 T}{\partial z^2}] \quad (5)$$

The boundary conditions used in the CFD code for solving the governing equations are shown in Table 1. An inlet velocity boundary condition is established for the front end of the fluid domain, whereas a pressure outlet boundary condition (0 gage pressure) is used for the rear end of the channel. Symmetric boundary conditions are specified at both side-ends of the flow path. Top and bottom surface are set to be adiabatic. The air inlet temperature was fixed at 310.6 K for all simulations. Usually in a tube-fin heat exchanger, due to the higher heat transfer coefficient inside the tube and high thermal conductivity of the tube wall, the temperature of tube surface can be considered as constant, which is set as 291.7 K to represent the working condition of heat exchanger for air conditioning applications [11].

2.3 Numerical methods, mesh generation, and validation

The Navier-Stokes and energy equations with the boundary condition equations are solved by using a computational fluid dynamics code (ANSYS FLUENT 15) based on finite volume methodology. The algorithm used for pressure-velocity coupling is SIMPLE (semi-implicit method for pressure-linked equations), which is widely used in numerical simulation of heat exchangers. The SIMPLE algorithm uses a relationship between velocity and pressure corrections to enforce mass conservation and to obtain the pressure field. Spatial discreti-

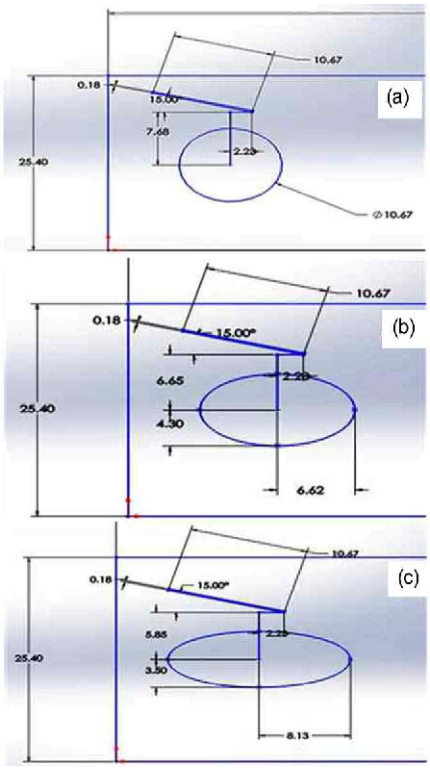

Fig. 4. Dimensions of the tubes and vortex generators at 15° angle of attack for (a) circular tubes, and for oval tubes with an aspect ratio (AR); (b) 1.54; (c) AR = 2.32.

zation of the momentum and energy equations was done by second-order upwind scheme and the gradient was Least squares cell based. The velocity formulation was absolute with a second-order spatial discretization of pressure. Multi-dimensional linear reconstruction approach is used in calculating the quantities of all cells in order to achieve second-order accuracy. The pressure-based solver is used to solve the governing equations with boundary conditions. Standard solution initialization was computed from the inlet. For solution control, under-relaxation factors for pressure, momentum and energy was 0.3, 0.7, and 1. The convergence criterion for the continuity, velocities is that the absolute criteria of residual is 0.001 and the convergence criterion for the energy is that the maximum value of the absolute criteria is 1.0×10^{-6}.

Standard meshing technique was adopted using ANSYS ICEM with high smoothing and default inflation settings. The entire domain is subdivided into discrete control elements, as shown in Fig. 5. In order to verify the grid independence of the numerical simulations conducted, several grid systems were examined, which is shown in Fig. 6. Among the different grid systems, the change in the averaged Nu number is less than 0.88 %. Based on this analysis, the grid number selected for the present study had 389669 cells. The computational cost for performing a simulation was typically 4-5 hours for a specific Re, on an 8.00 GB RAM, Intel(R) CORE(TM) i5-4200M CPU@ 2.50 GHz.

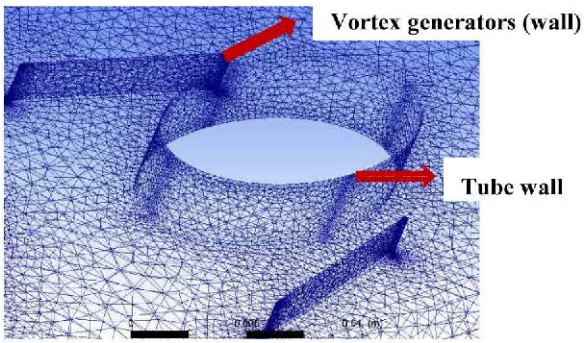

Fig. 5. The mesh refined computational domain.

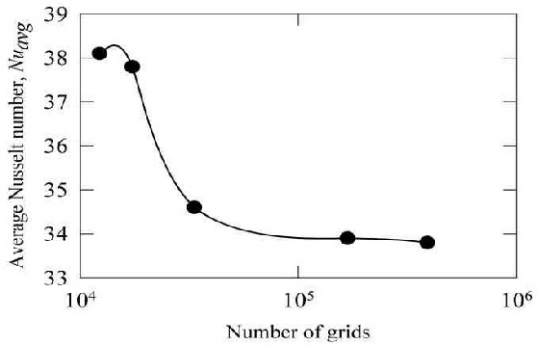

Fig. 6. Findings of the grid independence test.

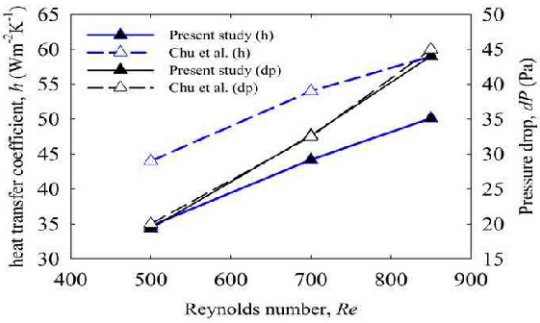

Fig. 7. Validation of the present model for the pressure drop and heat transfer coefficient with the germane work Chu et al. [15].

In addition, the reliability of the present numerical model is validated against the germane numerical work by Chu et al. [11] on a HE with the same geometric configuration. The simulated results on the pressure loss penalty (ΔP) and heat transfer coefficient hair of the air-side obtained in the present study are compared with the results from Chu et al. [11] and are shown in Fig. 7. It can be seen that the average discrepancy between the previously reported pressure loss and heat transfer coefficient values and the present numerical model is less than 1 % and 20 %, respectively. The obtained good agreement between these finding indicates the reliability of the present model in predicting the flow structure and heat transfer characteristics accurately.

The parameters - Reynolds number (Re), Nusselt number

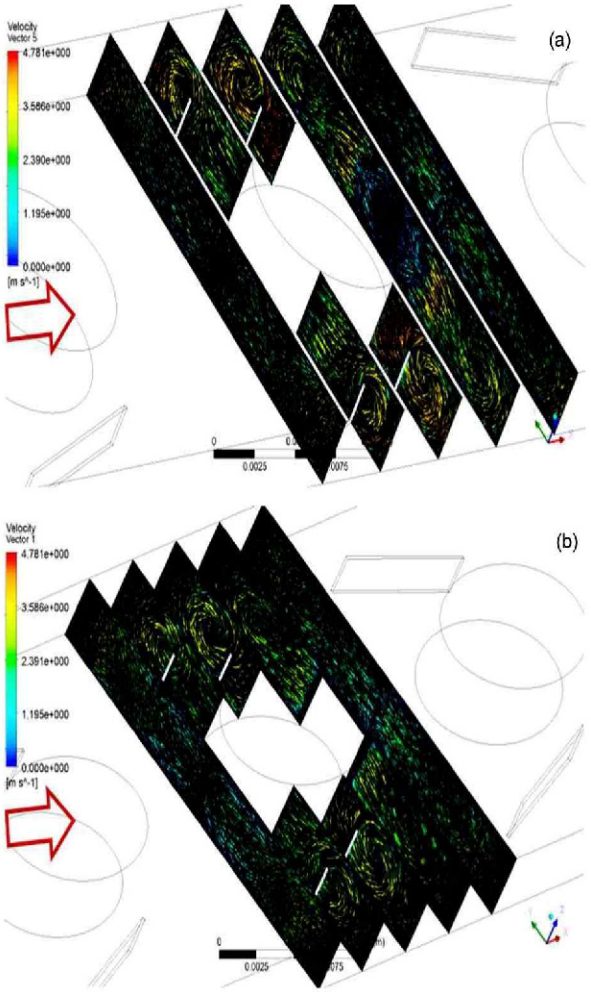

Fig. 8. Longitudinal vortices for CFU configuration of (a) circular tubes; (b) oval tube (AR = 1.80) at different cross-sections (x = 80, 85, 90, 95, 100 mm) at an angle of attack of 15º and 7RWPs.

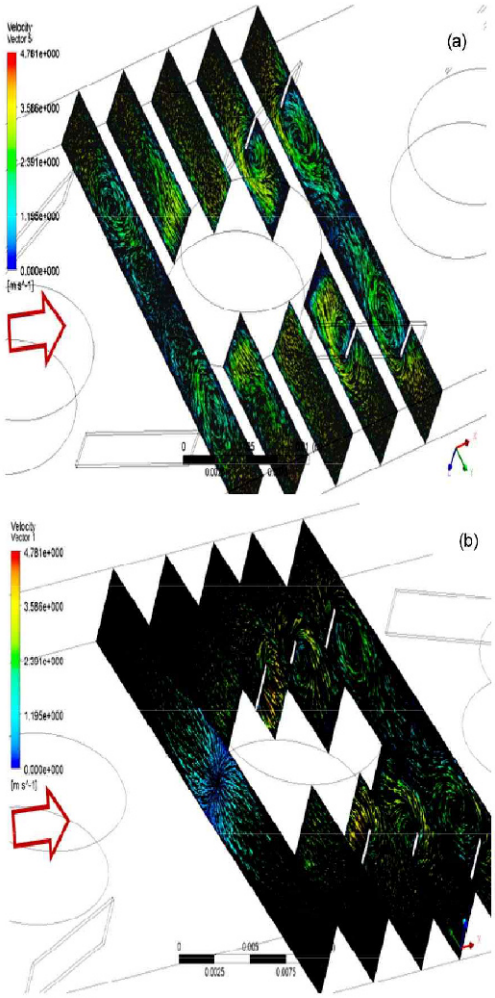

Fig. 9. Longitudinal vortices for (a) CFD configuration; (b) for (CFU+CFD) configuration at different cross-sections (x = 80, 85, 90, 95, 100 mm) of oval tubes with aspect ratio of = 1.80, at an angle of attack 15º and 7RWPs.

(Nu), heat transfer coefficient (h), Colburn factor (j), Friction factor coefficient (f), Area goodness factor (j/f), and Stanton number (St) [11] were calculated to post-process the results.

3. Results and discussion

3.1 Effects of the configuration of vortex generators

The effects of the common flow down (CFD) and the common flow up (CFU) configuration of LVGs with rectangular winglet pair (n-RWP, n = number of winglet pair) is studied at various Re. The CFU configuration shows a better overall performance than the CFD and (CFU+CFD)-staggered configuration for the RWP. Due to the pressure difference and frictional flow effects, longitudinal vortices are generated behind the winglet pairs. As the induced span-wise velocity of longitudinal vortices is considerably higher than that of the frontal velocity, they transport the fluid from the wake region of the tubes to the main flow regions, promoting enhanced mixing of the bulk fluid. The development of the secondary flow obtained from the simulations is presented at five different locations along the streamwise direction downstream of the LVGs for Re = 850. All the contours represent the development of the counter-rotating vortices by the LVGs, their subsequent deformation, and reduction of strength as the vortices move downstream in the channel.

The effects of channel walls on vertical structures can be realized when the cross flow at any two sections of the winglets is compared. The primary counter-rotating vortices result in the massive churning of the fluids from the channel wall to the central part of the tube. The circular tubes show a better heat transfer coefficient due to the high velocity-induced flow near the tube wall than the oval tubes. In the CFU configuration, the left winglet forms counter-clockwise rotating vortices, and the right winglet forms clockwise rotating vortices, as shown in Fig. 8. Subsequently, the distance between the core of the vortices decreases and the interaction between the counter-rotating vortex pairs increases considerably as a result. It is also

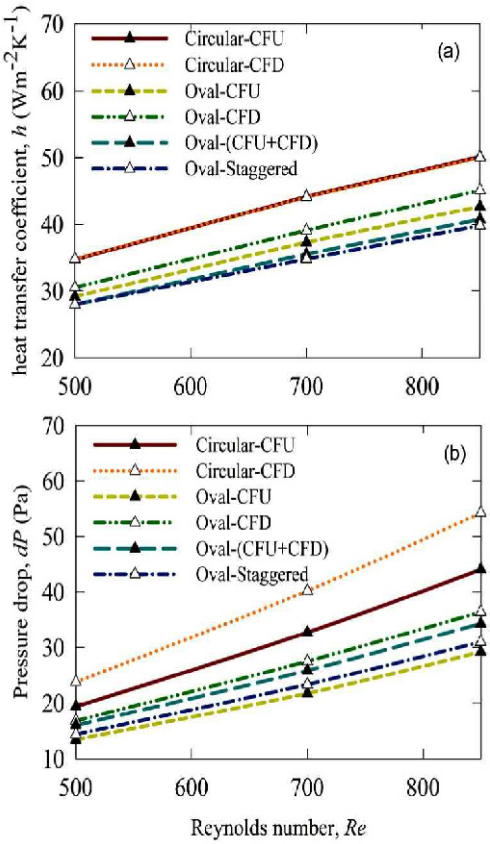

Fig. 10. Variations in (a) heat transfer coefficient; (b) pressure drop for a range of Re numbers at the different configuration of VGs for 7RWPs.

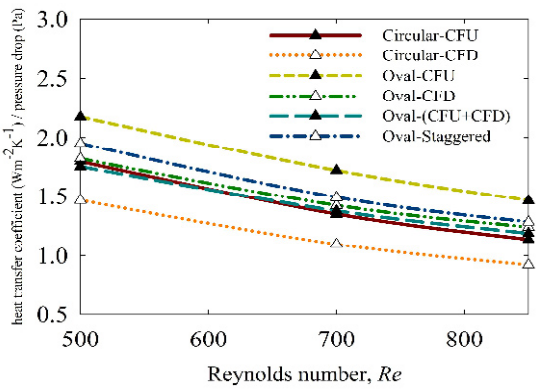

Fig. 11. Comparison of heat transfer coefficient with per unit pressure drop for different configuration of the VGs and tube shapes demonstrates a better performance of the oval tubes in CFU configuration.

observed that the core of the vortices in CFU gradually moves from the lower wall to the upper wall as the flow moves downstream. The thinning of the thermal boundary layer is on the outer region of the vortices. On the contrary, for the CFD configuration, the left winglet forms clockwise rotating vortices while the right winglet forms counter-clockwise rotating vortices along with the flow, as shown in Fig. 9. In this case, the thermal boundary sub-layer thins due to the decrease of secondary

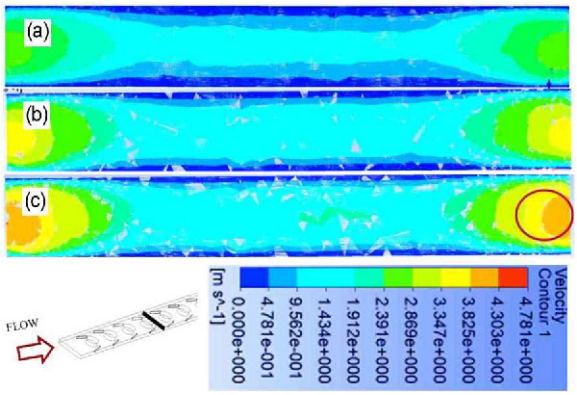

Fig. 12. Velocity contours for circular tubes at a plane, X = 98 mm for 7 VG configuration for (a) Re = 500; (b) Re = 700; (c) Re = 850 at an angle of attack of 15º.

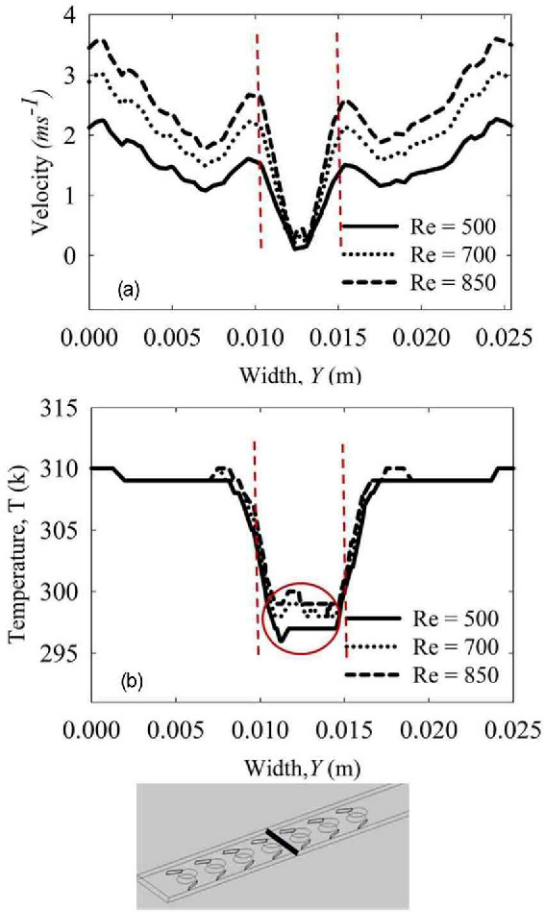

Fig. 13. (a) Velocity; (b) temperature distribution along the midline of YZ plane at a distance X = 98 mm for oval tubes (AR = 1.80) at different Re and 15º angle of attack.

flow vectors in between the developed vortices. Circular tube with VGs in a CFU configuration shows a better heat transfer ability than oval tubes in CFU configuration because of more intensification of the mixing motion (Fig. 10). Due to a manifested reduction in pressure drop penalty, the overall performance of

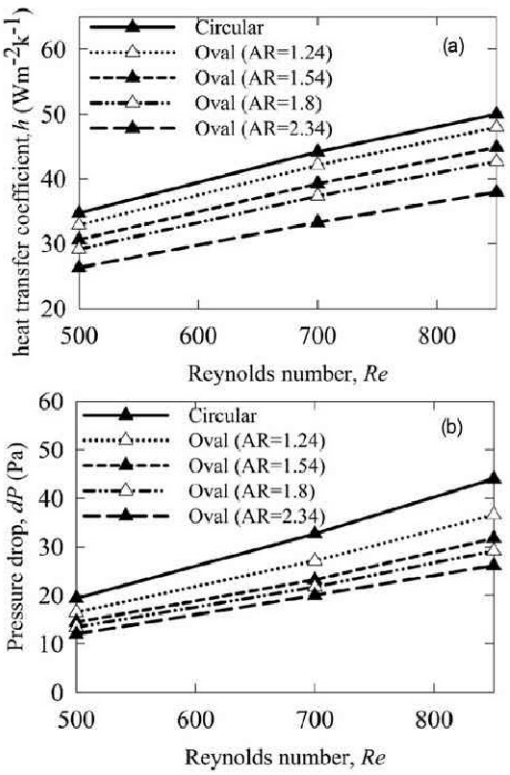

Fig. 14. Comparison of (a) heat transfer coefficient; (b) pressure drop with Re for different aspect ratios of oval tubes and that of circular tubes at a 15º angle of attack and 7RWPs.

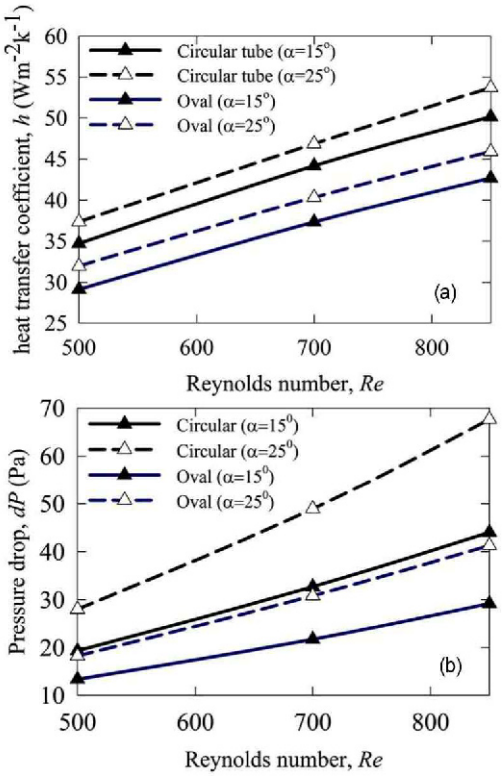

Fig. 15. Variation of (a) heat transfer coefficient; (b) pressure drop with Re for an angle of attacks of 15º and 25º for both circular and oval tube.

the oval tube is better than the circular tubes for all the *Re*, as can be seen from Fig. 10(b). For a more meaningful insight into the relative performance, heat transfer per unit pressure drop is shown in Fig. 11. It can be noted that oval tubes with seven VGs in a CFU configuration yield the optimum output if the pressure drop penalty is considered.

3.2 Effect of Re

The velocity contours at a prescribed plane are shown in Fig. 12 to illustrate the effects of the Re on the flow and heat transfer characteristics. Increasing Re predictably results in a higher velocity of the fluid as observed from the colored region (brown circle) seen in this contour plot. In this region, more fluid is flushed from the hot wall side to the central cooled tube region, intensifying the mixing significantly. Hence, heat transfer is greatly enhanced. Line averaged velocity, and temperature distribution is reported in Fig. 13 for further characterizing the effects of Re. The fluid is at a higher temperature compared to the tube wall (imposed boundary conditions), as result, the fluid temperature decreases at the tube wall, However, due to the symmetry boundary conditions (no thermal gradient) at the side walls or edges, the fluid temperature is same as that of the inlet temperature.

The peak fluid flow velocity is obtained at Re = 850. Stagnant points are located on the tube surface while velocity increases towards the wall of the channel. However, variation in temperature at the tube surface with Re is evident (circle marked). The temperature goes to approximately 300 K near the tube surface at Re = 850, indicating the highest possible heat transfer augmentation. For all the aspect ratios of oval tubes considered, an increase in Re increases both the heat transfer coefficient and pressure drop, as can be seen from Fig. 14. Although the circular tubes with vortex generators provide greater enhancement of heat transfer than oval tubes with higher aspect ratios, the overall performance of oval tubes with AR = 1.8 and 2.3 is better than that of circular tubes when the pressure drop penalty is considered. The pressure drop is reduced due to the reduction of form drag of the oval tube by its shape. However, decrement of the aspect ratio of the oval tubes presents more frontal area to the normal, incoming flow and induces more contact-area with the tube surfaces.

Furthermore, for simplicity, h/p ratio is defined as the heat transfer coefficient per unit pressure drop in Wm-2k-1/Pa unit to gain an estimate of heat transfer enhancement for different cases. It is observed that oval tubes with AR = 1.8 yield a heat transfer coeffi-cient of h = 43 Wm-2k-1 at a pressure drop of 28 Pa (h/p = 1.54) while circular tube yields a ratio of h/p = 1.14 for the same scenario. Circular tube with a 25º angle of attack exhibits a higher heat transfer ability than oval tubes due to the high volumetric flow rate of the fluid through the narrow passage. However, as explained before, if the pressure drop penalty is considered, the oval tubes exhibit superior overall per-

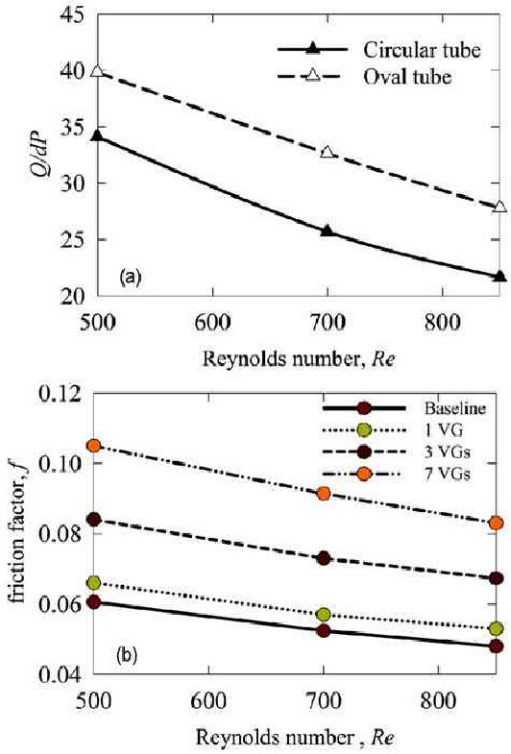

Fig. 16. (a) Simplified performance parameter, defined as the heat flux per unit pressure drop, for the circular and oval tubes demonstrate the suitability of oval tubes at low Re number applications; (b) a decreasing friction factor with Re number at the 15º angle of attack for oval tubes.

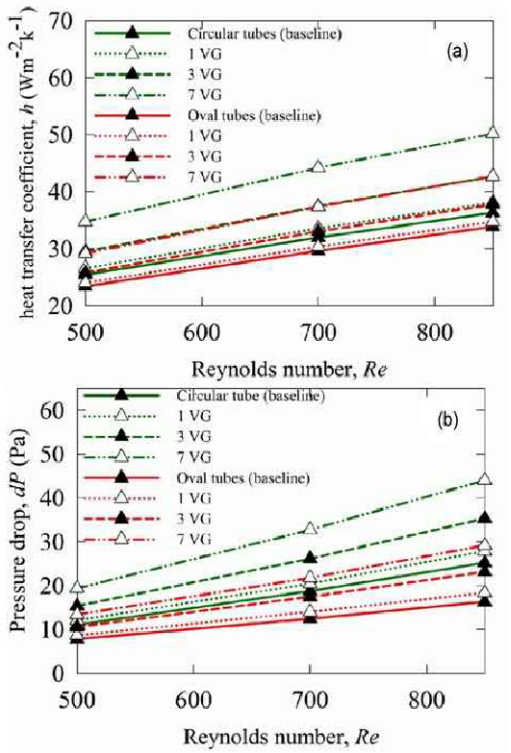

Fig. 17. Variation of h and pressure drop with Re.

formance. From Fig. 15, oval tubes with an angle of attack of 15° yields h = 42.5 Wm-2k-1 with a pressure drop of 29 Pa (h/p = 1.47) at Re = 850. In comparison, circular tubes with the same angle of attack result in slightly higher heat transfer coefficient of h = 50 Wm-2k-1with a considerably higher pressure drop of 40 Pa (h/p = 1.25) at the same Re. Regardless of the shape of the tube, the increase of the frontal area of winglet caused by the higher angle of attack plays a vital role in increasing the pressure drop. In order to obtain an improved understanding of the impact of the angle of attack of the VGs on the circular and oval tube banks, variation of the simplified performance parameter (heat flux per unit pressure drop) with Reynolds number is also analyzed (Fig. 16). It is seen that an increasing Reynolds number decreases this performance parameter for both circular and oval tubes. Oval tube yields a higher value (= 40) of the performance parameter at Re = 500 than the circular tube (Fig. 16(a)) under the same condition, demonstrating its potential in low Re applications. At the same time, as the Re increases, friction factor gradually decreases for all the stated cases (Fig. 16(a)). Higher Re implies a lower viscous force, thereby lower shear stress and hence a lower friction factor.

3.3 Effect of the number of VGs

As the number of VG increases, the bulk fluid mixing increases at each subsequent tube, transferring heat more effectively and hence yielding an enhancement of the heat transfer performance. As a result, the heat transfer coefficient for both circular and oval tube banks is found to increase with an increase of the VGs for the present study (Fig. 17).

For the calculation of area goodness factor (j/f), the Colburn factor (j) and the friction factor (f) is deduced from the Eq. (6) [11].

$$j = St.\mathrm{Pr}^{\frac{2}{3}}, f = \frac{\Delta P}{\frac{\rho V_m^2}{2}\cdot\frac{A_T}{A_{\min}}} \quad (6)$$

where St is the Stanton number, Pr is the Prandtl number, ΔP is the simulated pressure drop, V_m is the mean velocity of the flow, A_T is the total heat transfer surface area, and A_{min} is the minimum flow cross-section area.

Tube banks with 1VG are found to have a higher area goodness factor compared to the same with a higher number of vortex generator under the same operating condition. Although circular tube exhibits a higher heat transfer enhancement compared to the oval tubes for the same number of VGs, the pressure drop also increases. For circular tubes, the greater contact volume between mixing fluid results in a higher heat transfer coefficient. At the same time, the narrow passages of the fluid flow might give rise to a jet impingement effect and hence increased pressure drop. Additionally, the oval tube with 7 VGs

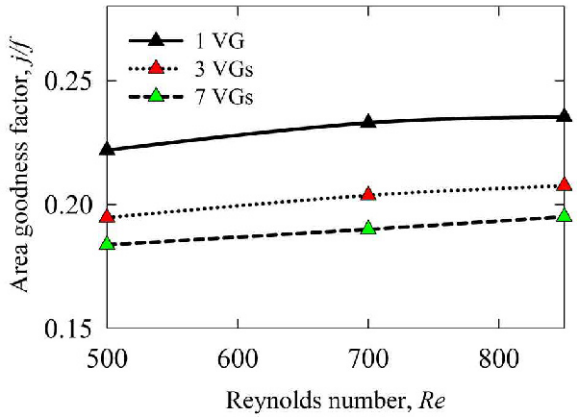

Fig. 18. Variation of area goodness factor with Re.

de-monstrates similar heat transfer to circular tubes with 3 VGs, but at a reduced pressure drop penalty.

3.4 Comparison of area goodness factor

Finally, the criterion of area goodness factor j/f is employed to evaluate the overall performance of the present HE with different tube arrangements, as shown in Fig. 18. For a specified range of Re (500-850), it is found that the area goodness factor j/f is about 15 % and 25 % higher for the 1-RWP over the 3-RWP and 7-RWP cases, respectively. The influence of the number of VGs on heat transfer, for both circular and oval tubes, decreases as it becomes gradually more dominant on pressure drop increment. In terms of the area goodness factor, the 1-RWP and 3-RWP cases indicate a smaller frontal area than the other combinations and hence would be more efficient and effective in HE design.

It can be noted that oval tubes with seven VGs in a CFU configuration yield the optimum output if the pressure drop penalty is considered.

4. Conclusions

This study presents the findings of a numerical investigation to examine the effect of VGs for turbulent flow through a fin-and-tube HE, using different geometric configurations of winglets and tubes. The tube shape, aspect ratios of oval tubes, Re, number of winglets, angle of attack of the winglets are varied to determine an optimal configuration of LVG for circular and oval tube banks for heat transfer enhancement. The main conclusions are drawn as follows:

(1) The circular tube (7VG) demonstrates nearly 45 % enhancement of heat transfer coefficient with an associated pressure drop penalty of 127 %.

(2) For oval tube banks, oval tubes with an aspect ratio of 1.25 provide a heat transfer enhancement of 27 % with about 70 % increase in the pumping power compared to the oval tube having an aspect ratio of 2.35.

(3) In terms of area goodness, the 1-RWP and 3-RWP cases would need a comparatively smaller frontal area of the tube than the other combinations considered and would be more advantageous in fin-and-tube HE design.

Very few studies could be found in the open literature on the effect of different design parameters on the thermo-hydraulic performance of multi-row fin-tube HE with VGs having oval tubes and circular tubes with the comparable cross-sectional area. Therefore, from a design guideline point of view to obtain an optimum configuration with oval tubes and VGs, a higher number of winglets at a high angle of attack, oval tubes with lower aspect ratio in a high Re flow could be preferred for higher heat transfer enhancement with a minimum rise in pressure drop.

Acknowledgments

This work was supported by the Mechanical engineering department of Bangladesh University of Engineering and Technology, Bangladesh.

Nomenclature

A_T	: Total heat transfer surface area
A_{min}	: Minimum flow cross section area
C_p	: Specific heat
f	: Friction factor
h	: Heat transfer coefficient
j	: Colburn factor
j / f	: Area goodness factor
K_f	: Thermal conductivity of fluid
Nu	: Nusselt number
Pr	: Prandtl number
P	: Pressure
Re	: Reynolds number
St	: Stanton number
T	: Temperature
u	: Velocity component along X-direction
v	: Velocity component along Y-direction
V_m	: Mean velocity
w	: Velocity component along Z-direction
ρ	: Density of fluid
μ	: Viscosity of the fluid

References

[1] S. A. E. S. Ahmed, O. M. Mesalhy and M. A. Abdelatief, Flow and heat transfer enhancement in tube heat exchangers, *Heat and Mass Transfer*, 51 (11) (2015) 1607-1630.

[2] S. Tiggelbeck, N. K. Mitra and M. Fiebig, Comparison of wing-type vortex generators for heat transfer enhancement in channel flows, *ASME. J. Heat Transfer*, 116 (4) (1994) 880-885.

[3] M. Fiebig, A. Valencia and N. K. Mitra, Wing-type vortex generators for fin-and-tube heat exchangers, *Exp. Therm. Fluid Sci.*, 7 (4) (1993) 287-295.

[4] M. Fiebig, Vortices, generators and heat transfer, *Chem. Eng.*

Sci., 76 (2) (1998) 108-123.

[5] S. Lau, K. Meiritz and V. I. V. Ram, Measurement of momentum and heat transport in the turbulent channel flow with embedded longitudinal vortices, *Int. J. Heat Fluid Fl.*, 20 (2) (1999) 128-141.

[6] K. Kwak, K. Torii and K. Nishino, Simultaneous heat transfer enhancement and pressure loss reduction for finned-tube bundles with the first or two transverse rows of built-in winglet, *Exp. Therm. Fluid Sci.*, 29 (5) (2005) 625-632.

[7] A. D. Sommers and A. M. Jacobi, Air-side heat transfer enhancement of a refrigerator evaporator using vortex generation, *Int. J. Refrig*., 28 (7) (2005) 1006-1017.

[8] S. Pesteei, P. Subbarao and R. Agarwal, Experimental study of the effect of winglet location on heat transfer enhancement and pressure drop in fin-tube heat exchangers, *Appl. Therm. Eng.*, 25 (11) (2005) 1684-1696.

[9] P. A. Sanders and K. A. Thole, Effects of winglets to augment tube wall heat transfer in louvered fin heat exchangers, *Int. J. Heat Mass Transfer*, 49 (21) (2006) 4058-4069.

[10] S. Hiravennavar, E. Tulapurkara and G. Biswas, A note on the flow and heat transfer enhancement in a channel with built-in winglet pair*, Int. J. Heat Fluid Fl.*, 28 (2) (2007) 299-305.

[11] P. Chu, Y. He and W. Tao, Three-dimensional numerical study of flow and heat transfer enhancement using vortex generators in fin-and-tube heat exchangers, *ASME. J. Heat Transfer*, 131 (9) (2009) 091903.

[12] A. Joardar and A. M. Jacobi, Heat transfer enhancement by winglet-type vortex generator arrays in compact plain-fin-and-tube heat exchangers, *Int. J. Refrig*., 31 (1) (2008) 87-97.

[13] J. S. Leu, Y. H. Wu and H. Y. Jang, Heat transfer and fluid flow analysis in plate-fin and tube heat exchangers with a pair of block shape vortex generators, *Int. J. Heat Mass Transfer*, 47 (19-20) (2004) 4327-4338.

[14] J. M. Wu and W. Q. Tao, Investigation on laminar convection heat transfer in fin-and-tube heat exchanger in aligned arrangement with longitudinal vortex generator from the viewpoint of field synergy principle, *Appl. Therm. Eng*., 27 (14-15) (2007) 2609-2617.

[15] S. W. Hwang, D. H. Kim, J. K. Min and J. H. Jeong, CFD analysis of fin tube heat exchanger with a pair of delta winglet vortex generators, *J. Mech. Sci. Technol.,* 26 (9) (2012) 2949-2958.

[16] Y. H. Zhang, X. Wu, L. B. Wang, K. W. Song, Y. X. Dong and S. Liu, Comparison of heat transfer performance of tube bank fin with mounted vortex generators to tube bank fin with punched vortex generators, *Exp. Thermal Fluid Sci.*, 33 (1) (2008) 58-66.

[17] Y. L. He and Y. Zhang, Chapter two - advances and outlooks of heat transfer enhancement by longitudinal vortex generators, *Advances in Heat Transfer,* 44 (2012) 119-185.

[18] Y. Chen, M. Fiebig and N. K. Mitra, Conjugate heat transfer of a finned oval tube with a punched longitudinal vortex generator in form of a delta winglet - parametric investigations of the winglet, *Int. J. Heat Mass Transfer*, 41 (23) (1998) 3961-3978.

[19] Y. Chen, M. Fiebig and N. K. Mitra, Heat transfer enhancement of a finned oval tube with punched longitudinal vortex generators in-line, *Int. J. Heat Mass Transfer*, 41 (24) (1998) 4151-4166.

[20] Y. Chen, M. Fiebig and N. K. Mitra, Heat transfer enhancement of finned oval tubes with staggered punched longitudinal vortex generators, *Int. J. Heat Mass Transfer*, 43 (3) (2000) 417-435.

[21] S. Tiwari, D. Maurya, G. Biswas and V. Eswaran, Heat transfer enhancement in cross-flow heat exchangers using oval tubes and multiple delta winglets, *Int. J. Heat Mass Transfer*, 46 (15) (2003) 2841-2856.

[22] V. Prabhakar, G. Biswas and E. Eswaran, Numerical prediction of heat transfer in a channel with a built-in oval tube and two different shaped vortex generators, *Numer. Heat Tr. A-Appl.*, 41 (3) (2002) 307-329.

[23] V. Prabhakar, G. Biswas and E. Eswaran, Numerical prediction of heat transfer in a channel with a built-in oval tube and various arrangements of the vortex generators, *Numer. Heat Tr. A-Appl*., 44 (3) (2003) 315-333.

[24] J. E. O'Brien and M. S. Sohal, Local heat transfer for finned-tube heat exchangers using oval tubes, *Proc. of 2000 ASME National Heat Transfer Conference*, Pittsburgh, New York, USA (2000).

[25] J. E. O'Brien, M. S. Sohal and P. C. Wallstedt, Local heat transfer and pressure drop for finned-tube heat exchangers using oval tubes and vortex generators, *ASME. J. Heat Transfer*, 126 (5) (2004) 826-835.

[26] W. Jedsadaratanachai and A. Boonloi, Thermal performance assessment in a fin-and-oval-tube heat exchanger with delta winglet vortex generators, *J. Mech. Sci. Technol*., 29 (4) (2015) 1765-1779.

[27] M. Oneissi, C. Habchi, S. Russeila, T. Lemenandb and D. Bougeard, Heat transfer enhancement of inclined projected winglet pair vortex generators with protrusions, *Int. J. Therm. Sci.*, 134 (2018) 541-551.

[28] L. H. Tang, W. X. Chu, N. Ahmed and M. Zeng, A new configuration of winglet longitudinal vortex generator to enhance heat transfer in a rectangular channel, *Appl. Therm. Eng.*, 104 (2016) 74-84.

[29] A. Boonloi and W. Jedsadaratanachai, Flow topology, heat transfer characteristic and thermal performance in a circular tube heat exchanger inserted with punched delta winglet vortex generators, *J. Mech. Sci. Technol*., 30 (1) (2016) 457-471.

[30] S. Tamna, Y. Kaewkohkiat, S. Skullong and P. Promvonge, Heat transfer enhancement in tubular heat exchanger with double V-ribbed twisted-tapes, *Case Studies in Thermal Eng.,* 7 (2016) 14-24.

[31] H. E. Ahmed, M. Z. Yusoff, M. N. A. Hawlader, M. I. Ahmed, B. H. Salman and A. S. Kerbeet, Turbulent heat transfer and nanofluid flow in a triangular duct with vortex generators, *Int. J. Heat Mass Transfer,* 105 (2017) 495-504.

[32] X. H. Wu, P. Yuan, Z. M. Luo, L. X. Wang and Y. L. Lu, Heat transfer and thermal resistance characteristics of fin with built-in interrupted delta winglet type, *Heat Transfer Eng*., 37 (2) (2016) 172-182.

[33] L. Garelli, G. L. Rodriguez, J. J. Dorella and M. A. Storti, Heat transfer enhancement in panel type radiators using delta-wing vortex generators, *Int. J. Therm. Sci.*, 137 (2019) 64-74.
[34] K. W. Song and T. Tagawa, The optimal arrangement of vortex generators for best heat transfer enhancement in flat-tube-fin heat exchanger, *Int. J. Therm. Sci.*, 132 (2018) 355-367.
[35] S. A. E. S. Ahmed, O. M. Mesalhy and M. A. Abdelatief, Heat transfer characteristics and entropy generation for wing-shaped-tubes with longitudinal external fins in cross-flow, *J. Mech. Sci. Technol.*, 30 (6) (2016) 2849-2863.
[36] M. Nakhchi and J. Esfahani, Performance intensification of turbulent flow through heat exchanger tube using double V-cut twisted tape inserts, *Chem. Eng. and Processing-Process Intensification*, 141 (2019) 107533.
[37] F. Afshari, H. G. Zavaragh and G. Di Nicola, Numerical analysis of ball-type turbulators in tube heat exchangers with computational fluid dynamic simulations, *International Journal of Environmental Science and Technology*, 16 (7) (2019) 3771-3780.
[38] M. A. Abdelatief, S. A. E. S. Ahmed and O. M. Mesalhy, Experimental and numerical study on thermal-hydraulic performance of wing-shaped-tubes-bundle equipped with winglet vortex generators, *Heat and Mass Transfer*, 54 (3) (2018) 727-744.
[39] S. A. E. S. Ahmed, E. Z. Ibrahiem, O. M. Mesalhy and M. A. Abdelatief, Heat transfer characteristics of staggered wing-shaped tubes bundle at different angles of attack, *Heat and Mass Transfer*, 50 (8) (2014) 1091-1102.
[40] S. A. E. S. Ahmed, E. Z. Ibrahiem, O. M. Mesalhy and M. A. Abdelatief, Effect of attack and cone angels on air flow characteristics for staggered wing shaped tubes bundle, *Heat and Mass Transfer*, 51 (7) (2015) 1001-1016.
[41] K. W. Song, Z. P. Xi, M. Su, X. Wu and L. B. Wang, Effect of geometric size of curved delta winglet vortex generators and tube pitch on heat transfer characteristics of fin-tube heat exchanger, *Exp. Therm. Fluid Sci.*, 82 (2017) 8-18.
[42] E. N. Amanifard and H. M. Deylami, Comparison of simple and curved trapezoidal longitudinal vortex generators for optimum flow characteristics and heat transfer augmentation in a heat exchanger, *Appl. Therm. Eng.*, 125 (2017) 1414-1425.
[43] H. Naik, S. Harikrishnan and S. Tiwari, Numerical investigations on heat transfer characteristics of curved rectangular winglet placed in a channel, *Int. J. Therm. Sci.*, 129 (2018) 489-503.
[44] K. W. Song, T. Tagawa, Z. H. Chen and Q. Zhang, Heat transfer characteristics of concave and convex curved vortex generators in the channel of plate heat exchanger under laminar flow, *Int. J. Therm. Sci.*, 137 (2019) 215-228.
[45] J. Joseph, M. Delanaye, R. Nacereddine, A. Giraldo, M. Rouabah, J. G. Korvink and J. J. Brandner, Numerical and experimental investigation of a wire-net compact heat exchanger performance for high-temperature applications, *Appl. Therm. Eng.*, 154 (2019) 208-216.
[46] M. Mortean, L. Cisterna, K. Paiva and M. Mantelli, Thermal and hydrodynamic analysis of a cross-flow compact heat exchanger, *Appl. Therm. Eng.*, 150 (2019) 750-761.
[47] F. Silva and L. Salviano, Heat transfer enhancement in a flat-plate solar water heater through longitudinal vortex generator, *Journal of Solar Energy Engineering*, 141 (4) (2019) 041003.
[48] S. Ferrouillat, P. Tochon, C. Garnier and H. Peerhossaini, Intensification of heat-transfer and mixing in multifunctional heat exchangers by artificially generated streamwise vorticity, *Appl. Therm. Eng.*, 26 (16) (2006) 1820-1829.

Mohammad Rejaul Haque is working as a faculty member in MPE Dept. of Ahsanullah University of Science and Technology, Dhaka-1208, Bangladesh. He has recently received his Ph.D. degree from Kansas State University (USA). He received his B.Sc. and M.Sc. degrees in Mechanical Engineering from Bangladesh University of Engineering and Technology in 2013 and 2016, respectively. His research interest includes thermal energy, condensation and frosting, nano-micro scale fabrication, and CFD.

Md. Ashiqur Rahman is an Associate Professor of Department of Mechanical Engineering at Bangladesh University of Engineering and Technology (BUET). He received his Ph.D. degree from University of Illinois at Urbana-Champaign (USA). His research interest includes thermal sciences, energy systems and fire dynamics.